

**NASA Technical Memorandum 72846**

**Drag Reduction Obtained  
by Modifying a Standard Truck**

**Arthur E. Sheridan and Steven J. Grier**

**FEBRUARY 1978**



NASA Technical Memorandum 72846

# Drag Reduction Obtained by Modifying a Standard Truck

Arthur E. Sheridan and Steven J. Grier  
*Dryden Flight Research Center*  
*Edwards, California*



National Aeronautics  
and Space Administration

**Scientific and Technical  
Information Office**

1978

# DRAG REDUCTION OBTAINED BY MODIFYING A STANDARD TRUCK

Arthur E. Sheridan and Steven J. Grier  
Dryden Flight Research Center

## INTRODUCTION

The continuing increase in the prices of gasoline and diesel fuel coupled with the uncertainty about future supplies has created widespread interest in the efficiency of ground vehicles. Of special interest are high volume, "box-shaped" transports, such as delivery vans, trucks, and motor homes, which have high drag due to their especially poor flow characteristics.

Results of tests conducted on a box-shaped ground vehicle that simulated a motor home (refs. 1 and 2) showed that the aerodynamic drag can be reduced significantly through modifications to the box shape. The purpose of the present study was primarily to investigate whether significant incremental drag reductions could be realized with similar modifications to a box-shaped cargo compartment behind a standard cab. Modifications included rounding the forward edges and mounting a flow vane in various positions on the forward top edge.

## SYMBOLS

All dimensional values given in this report were measured or derived in U.S. Customary Units because all instrumentation was calibrated in that system. Final values were then converted to the International System of Units (SI) using the factors given in reference 3. Velocity is the only exception: Final values were converted to kilometers per hour instead of the SI unit, meters per second, because of the greater convenience of kilometers per hour in automotive application.

A            vehicle frontal cross-sectional area (does not include undercarriage and tires),  $7.8 \text{ m}^2$  ( $84 \text{ ft}^2$ )

$C_{D_a}$        aerodynamic drag coefficient,  $\frac{D_a}{qA}$

$D_a$	aerodynamic drag
$D_m$	mechanical drag
$D_t$	total drag
$D_{t_{av}}$	average total drag for each configuration and velocity interval
$\Delta D_t$	total drag difference, $D_t - D_{t_{av}}$
$F_i$	inertial thrust
$g$	local acceleration due to gravity, $9.795 \text{ m/sec}^2$ ( $32.137 \text{ ft/sec}^2$ )
$I_r$	rotational moment of inertia of all tires, wheels, and brake drums, $40.91 \text{ kg m}^2$ ( $30.14 \text{ slug ft}^2$ )
$m$	vehicle mass, $\frac{W}{g}$
$q$	dynamic pressure, $0.5 \rho V^2$
$R_o$	tire outside radius
$r$	radius of curvature, $0.49 \text{ m}$ ( $19 \text{ in.}$ )
$T$	ambient air temperature
$\Delta T$	temperature difference, $T - T_{av}$
$T_{av}$	average ambient air temperature for each configuration
$\Delta t$	time increment
$V$	velocity
$\Delta V$	velocity increment
$W$	vehicle weight
$w$	cargo compartment width
$\alpha$	angular acceleration of wheels
$\rho$	air density

## TEST VEHICLE AND CONFIGURATIONS

### Test Vehicle

The basic test vehicle (fig. 1) was a 1966 Chevrolet, two-axle, cab-behind-engine truck with a model 60 cab and a box-shaped cargo compartment. (The vehicle used in this study was one of many that could have been used. The make and model are given for completeness only.) There was no gap between the cab and the cargo compartment. Geometric specifications are shown in figure 2. The vehicle had a net load capacity of 4990 kilograms (11,000 pounds); during testing, the average gross mass was 3706 kilograms (8170 pounds).

### Vehicle Configurations

Baseline configuration.—All the forward vertical and horizontal edges of the cargo compartment of the baseline configuration (configuration A) were square (fig. 1).

Configuration with rounded edges.—For configuration B (fig. 3), the forward top and side edges of the cargo compartment were rounded with a radius of curvature equal to 20 percent of the cargo compartment width ( $r = 0.48$  m (19 in.)). This radius was chosen based on previous work on the drag reduction of a box-shaped ground vehicle as reported in references 1 and 2.

Configurations with add-on flow vane.—For configurations C, D, and E, an add-on flow vane was located as shown in figure 4. The vane consisted of a curved sheet metal extension connected to the top forward edge of the cargo compartment and was attached in a slightly different fashion for each of the three configurations (fig. 5). The radius of curvature of the vane was the same as that of the rounded corners in configuration B—20 percent of the cargo compartment width. The angle subtended by the curved surface was  $64^\circ$ .

For configuration C, the flow vane was mounted flush with the forward edge of the cargo compartment upper surface. In configurations D and E, however, the surface of the vane did not attach directly to the forward upper edge of the cargo compartment. For configuration D, there was a 0.05-meter (2.0-inch) horizontal slot between the flow-vane surface and the front surface of the cargo compartment. Configuration E included a vertical gap measuring 0.05 meter (2.0 inches) between the upper surface of the cargo compartment and the vane surface.

## TEST METHOD

### Instrumentation

Deceleration was measured using a bank of five 0.1-second stopwatches and a calibrated precision speedometer with a 0.1-mile per hour readout capability. The

speedometer was driven by a fifth wheel (fig. 6). The values of velocity and distance were obtained from the fifth wheel and were displayed digitally inside the truck's cab (fig. 7). The time increments corresponding to preselected velocity intervals in miles per hour were obtained by starting all the stopwatches simultaneously at the starting test velocity and stopping them individually at the end of the desired velocity interval. The stopwatch data were recorded by hand at the end of each test run.

### Experimental Concept

In this study, the coastdown deceleration technique was used to determine the total drag of the vehicle. For the purposes of this paper, total drag\* is defined as the sum of aerodynamic and mechanical drag minus the thrust from the rotational inertia of the wheels, tires, and brake drums. The aerodynamic drag is then given by the equation

$$D_a = D_t - D_m + F_i = \left(\frac{\Delta V}{\Delta t}\right)m - D_m + F_i$$

Coastdown method.—Total drag,  $D_t$ , was measured using the coastdown deceleration method described in references 1, 2, 4, and 5. For this method, the vehicle was accelerated beyond the starting test velocity and then allowed to decelerate with the transmission in neutral. During deceleration, the time increments were measured for a series of predetermined velocity intervals of 8.05 kilometers per hour (5 miles per hour). These velocity intervals and time increments were used to calculate the average deceleration for each velocity interval. The average deceleration was then multiplied by the mass of the vehicle to obtain total drag.

Mechanical drag.—An analytical description of mechanical drag is beyond the scope of this study due to the large number of variables involved. Therefore, an endpoint value of mechanical drag was obtained experimentally at very low velocities, where aerodynamic drag and inertial thrust could be neglected, and an extrapolation was made for test velocities based on a semiempirical equation derived by Hoerner in reference 6.

The mechanical drag was determined at low velocities in two ways on each testing day. In the primary method, the coastdown technique was employed from 5 miles per hour to a complete stop, and the time increment was recorded for each 1-mile per hour velocity increment. In the backup method, the vehicle was towed by hand with a spring scale at a constant low velocity. The velocity was held constant by reference to the digital readout (fig. 7) of the fifth-wheel speedometer. Mechanical drag was read directly from the spring scale. Towing was done separately by two people on each test day. The average results of the towing and

---

\*Perhaps the term "net drag" would be more accurate here, but the term "total drag" was chosen for the sake of consistency with references 1, 2, 4, and 5. However, in references 1, 2, 4, and 5, the term "mechanical drag" refers to the difference between "mechanical drag" and "inertial thrust" as defined in this report.

coastdown methods were compared and a difference of 3.5 percent was determined. The final approximation showing mechanical drag as a function of velocity is presented in figure 8.

*Inertial thrust.*—Inertial thrust was calculated for the vehicle based on an approximation of the moment of inertia of the tires, wheels, and brake drums.\* Once the rotational moment of inertia of the tires and the wheel assemblies had been determined, inertial thrust was calculated for the vehicle at test velocities using the following equation:

$$F_i = \left( \frac{\alpha}{R_o} \right) I_r = \left( \frac{I_r}{R_o^2} \right) \left( \frac{\Delta V}{\Delta t} \right)$$

In figure 9, inertial thrust is shown as a function of velocity for each configuration.

#### Test Conditions

Test runs were made on the runway used to investigate the drag reduction of the box-shaped ground vehicle (refs. 1 and 2). This runway is exceptionally smooth and has an elevation gradient of only 0.08 percent; the effects of gradient and winds were eliminated by averaging runs made in opposite directions. Testing was cancelled when wind speeds exceeded 3 knots along the runway or 6 knots across the runway; however, most of the tests were made early in the day when winds were calm. When there were winds, the most common condition encountered was a crosswind of up to 3 knots. Test velocities ranged from 56.3 to 94.6 kilometers per hour (35 to 60 miles per hour).

On each day of testing, wind speed and direction and ambient pressure and temperature were monitored and documented every 15 minutes at the Edwards Air Force Base weather station so that the effects of these factors could be taken into account. Wind speed and direction were also monitored and documented at the runway after each test run using an anemometer. All reported drag data were corrected for ambient temperature differences, as described in the appendix. The vehicle was weighed, with occupants, after each day's testing to provide the proper mass for computing drag. The vehicle began each day of testing with a tire pressure of 2870 pascals (60 lb/in<sup>2</sup>).

---

\*This approximation was derived originally for airplane tires and wheels by Conway in reference 7 and was verified experimentally on the tires and wheels from the vehicles tested in references 1, 2, 4, and 5.

## RESULTS AND DISCUSSION

### Tuft Patterns

The tuft photographs shown in figures 10(a), 10(b), and 10(c) indicate the flow patterns along the top and sides of the cargo compartment for configurations A, B, and D, respectively. Tuft flow patterns for configurations C and E are not shown because they were very similar to the pattern for configuration D.

The photographs show that for the baseline configuration, configuration A, the flow on the sides and top of the cargo compartment is separated for the first one-half to two-thirds of the compartment. For the configuration with rounded edges, configuration B, the tuft patterns indicate attached flow from the forward edges of the corner radius through the entire length of the cargo compartment. The three configurations incorporating the flow vane, configurations C, D, and E, had attached flow on the top surface from the front edge of the vane to the rear of the cargo compartment. However, as would be expected, the flow on the sides of the compartment was similar to the baseline configuration: Because the forward side edges were unmodified, the flow remained separated over the first one-half to two-thirds of the surface.

### Drag Reduction

Total drag data for each configuration are presented in figure 11. The curve for each configuration is a fairing of the data using a least squares approximation method (ref. 8). The curves for all configurations are presented for comparison on the composite plot in figure 12.

The aerodynamic drag coefficients and the approximate reductions in aerodynamic and total drag at 88.5 kilometers per hour (55 miles per hour) are summarized in the following table.

Configuration	$C_{D_a}$	Aerodynamic drag reduction, percent	Total drag reduction, percent
A	0.875	---	---
B	0.610	30	26
C	0.808	8	7
D	0.815	7	6
E	0.794	9	8

The results given in the table indicate that for a speed of 88.5 kilometers per hour (55 miles per hour), rounding the top edge and the two vertical forward edges of the cargo compartment provided a 30 percent reduction in aerodynamic drag as compared to the baseline, configuration A. The rounding of these three forward edges prevented flow separation on the top and side surfaces of the compartment (fig. 10(a)) where the flow had been separated on configuration A (fig. 10(b)).



The average aerodynamic drag reduction provided by the flow vane was 8 percent as compared to the baseline, or 26 percent of that provided by rounding the front edges. All three flow-vane configurations prevented flow separation on the cargo compartment top surface (fig. 10(c)).

The forward edge length modified by the flow vane in configurations C, D, and E was determined to be equal to 30 percent of the edge length modified by rounding in configuration B. When this relationship was used to normalize the total length of the forward edge modified in each case, the effective drag reduction provided by rounding the forward edges was determined to be nearly the same as that provided by adding the flow vane.

#### CONCLUDING REMARKS

A standard two-axle truck with a box-shaped cargo compartment was tested using the coastdown method to determine whether significant reductions in aerodynamic drag could be obtained by modifying the cargo compartment. For the baseline configuration, all the cargo compartment corners and edges were square. The modifications investigated included the rounding of the forward top and side edges and the addition of a flow vane in various positions on the forward top edge of the cargo compartment. Test velocities ranged from 56.3 to 94.6 kilometers per hour (35 to 60 miles per hour).

At a velocity of 88.5 kilometers per hour (55 miles per hour), the configuration with rounded edges provided a 30 percent reduction in aerodynamic drag as compared to the baseline configuration. At the same velocity, the average aerodynamic drag reduction provided by the configurations having the flow vane attached to the top forward edge was 8 percent as compared to the baseline, or 26 percent of that provided by the configuration with rounded edges. These results suggest that if the flow-vane concept were applied to the forward vertical edges as well as the forward top edge, an aerodynamic drag reduction comparable to that provided by rounding the forward edges could be obtained. However, further testing would be needed for confirmation.

*Dryden Flight Research Center  
National Aeronautics and Space Administration  
Edwards, Calif., June 13, 1977*

## APPENDIX

### TEMPERATURE CORRECTION APPLIED TO TOTAL DRAG DATA

In analyzing the total drag data, it was noted that data taken on cold days indicated drag values systematically higher than the average value for each configuration and velocity interval, while data taken on warm days indicated drag values systematically lower than the average value.

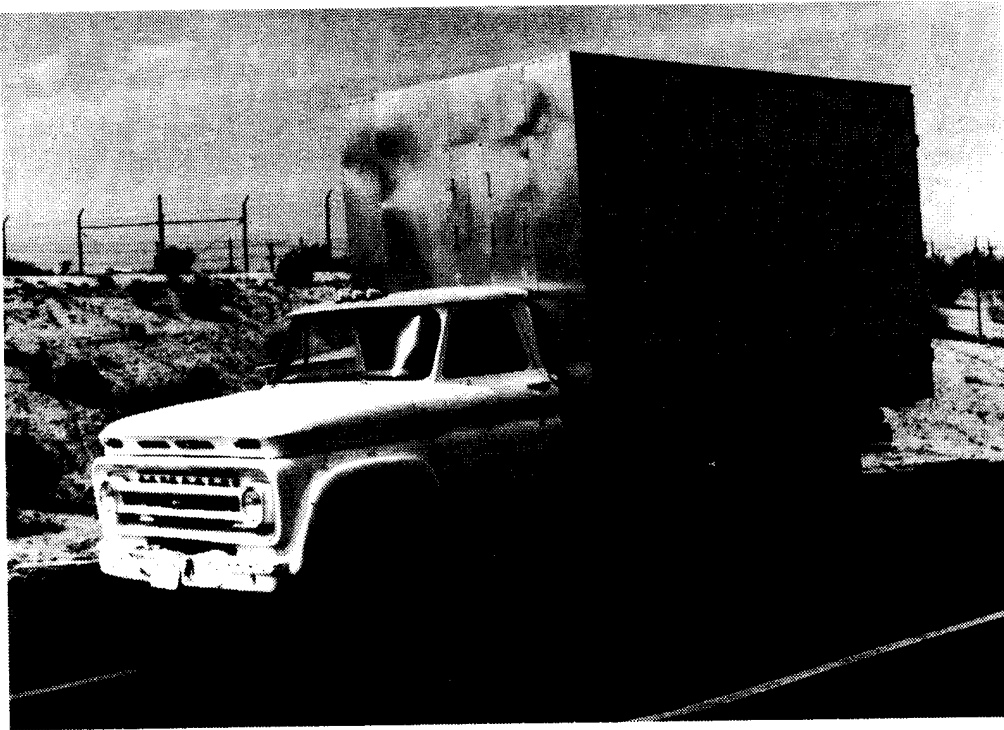
The ambient temperature variations in this study had only a small effect on dynamic pressure, which in turn had a very small effect on the total drag when compared to the differences noted above. Therefore, the dynamic pressure was not adjusted for temperature variations.

However, ambient temperature has been shown to have a pronounced effect on mechanical drag until the driveline components warm up, the warmup period being approximately the first 48 kilometers (30 miles) driven (ref. 9). Because the tests in this study were performed within such a warmup period, this effect is considered to account for most of the differences noted in the total drag data. Therefore, a temperature correction was applied.

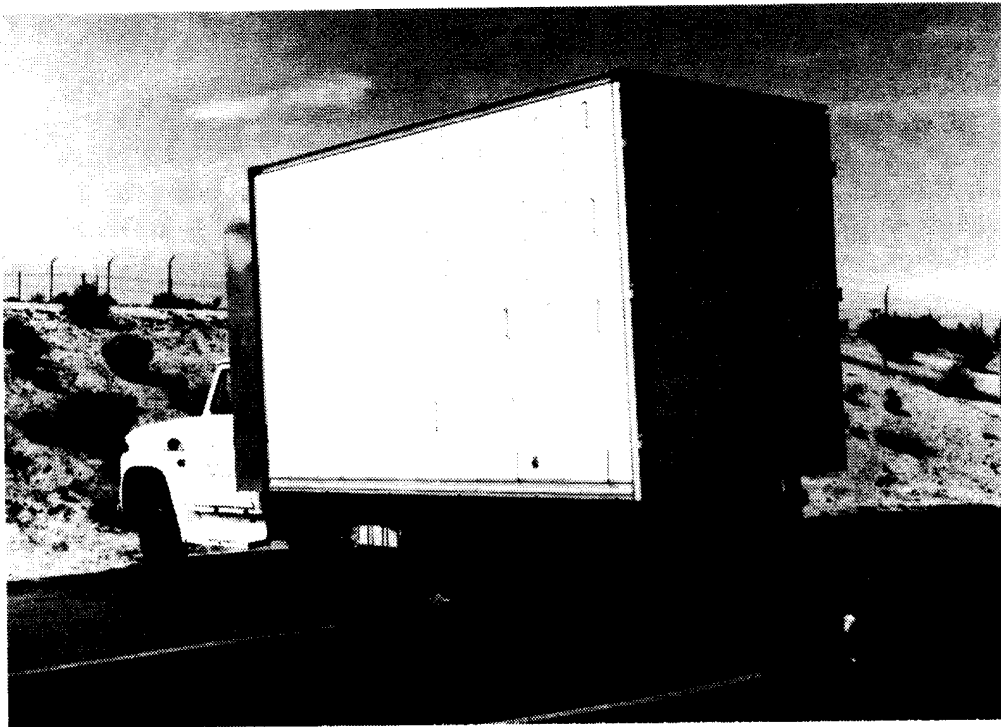
To apply the temperature correction, the average values for temperature and total drag were determined for each configuration and velocity interval. The difference between each measured value of total drag and the average was plotted versus the difference between each recorded value of temperature and the average (fig. 13). A straight line was then faired using the least squares approximation from reference 8. The final temperature correction determined from the slope of the line was  $11.2 \text{ N/}^\circ\text{C}$  ( $1.4 \text{ lbf/}^\circ\text{F}$ ). All total drag data were normalized to  $15.5^\circ \text{ C}$  ( $60^\circ \text{ F}$ ): Drag values determined at a temperature below  $15.5^\circ \text{ C}$  ( $60^\circ \text{ F}$ ) were decreased by  $11.2 \text{ N/}^\circ\text{C}$  ( $1.4 \text{ lbf/}^\circ\text{F}$ ) and drag values determined at a temperature above  $15.5^\circ \text{ C}$  ( $60^\circ \text{ F}$ ) were increased by  $11.2 \text{ N/}^\circ\text{C}$  ( $1.4 \text{ lbf/}^\circ\text{F}$ ).

## REFERENCES

1. Saltzman, Edwin J.; and Meyer, Robert R., Jr.: Drag Reduction Obtained by Rounding Vertical Corners on a Box-Shaped Ground Vehicle. NASA TM X-56023, 1974.
2. Saltzman, Edwin J.; Meyer, Robert R., Jr.; and Lux, David P.: Drag Reductions Obtained by Modifying a Box-Shaped Ground Vehicle. NASA TM X-56027, 1974.
3. Mechtly, E. A.: The International System of Units - Physical Constants and Conversion Factors. Second Revision. NASA SP-7012, 1973.
4. Montoya, Lawrence C.; and Steers, Louis L.: Aerodynamic Drag Reduction Tests on a Full-Scale Tractor-Trailer Combination With Several Add-On Devices. NASA TM X-56028, 1974.
5. Steers, Louis L.; Montoya, Lawrence C.; and Saltzman, Edwin J.: Aerodynamic Drag Reduction Tests on a Full-Scale Tractor-Trailer Combination and a Representative Box-Shaped Ground Vehicle. SAE Paper 750703, 1975.
6. Hoerner, Sigward F.: Fluid-Dynamic Drag. Publ. by the author (148 Busted Dr., Midland Park, N.J.), 1965.
7. Conway, H. G.: Landing Gear Design. Chapman and Hall, Ltd., 1958, p. 52.
8. Graybill, Franklin A.: An Introduction to Linear Statistical Models. Volume I. McGraw-Hill Book Co., Inc., 1961.
9. Burke, Carl E.; Nagler, Larry H.; Campbell, E. C.; Zierer, W. E.; Welch, H. L.; Lundstrom, L. C.; Kosier, T. D.; and McConnell, W. A.: Where Does All the Power Go? SAE Transactions, Vol. 65, 1957, pp. 713-738.



E-32262



E-32259

*Figure 1. Baseline vehicle, configuration A.*

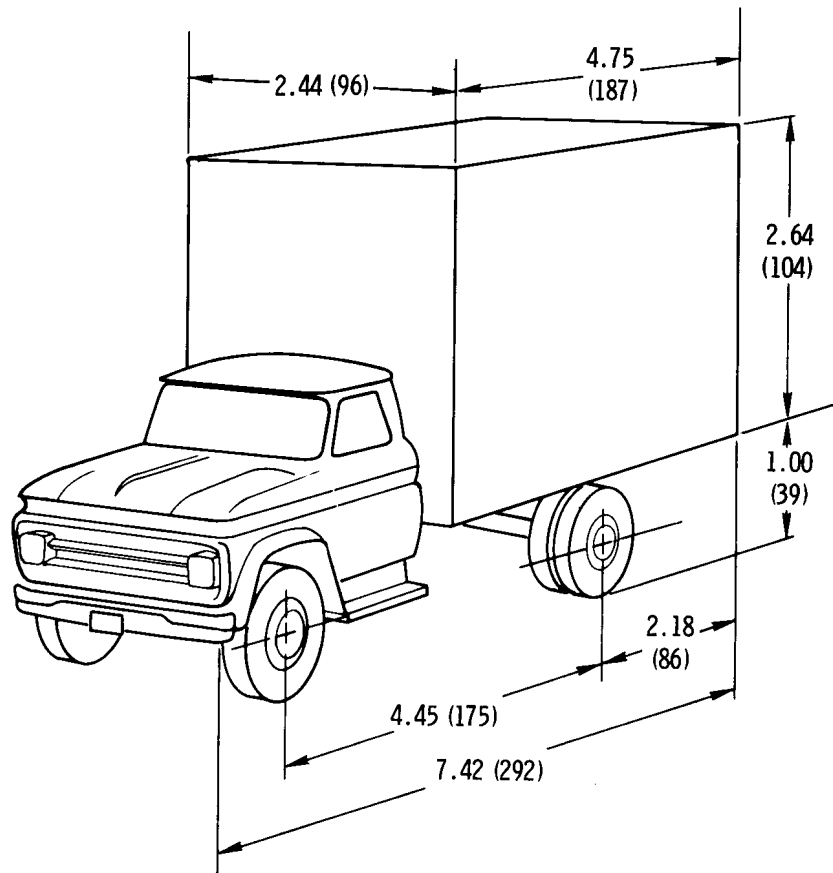
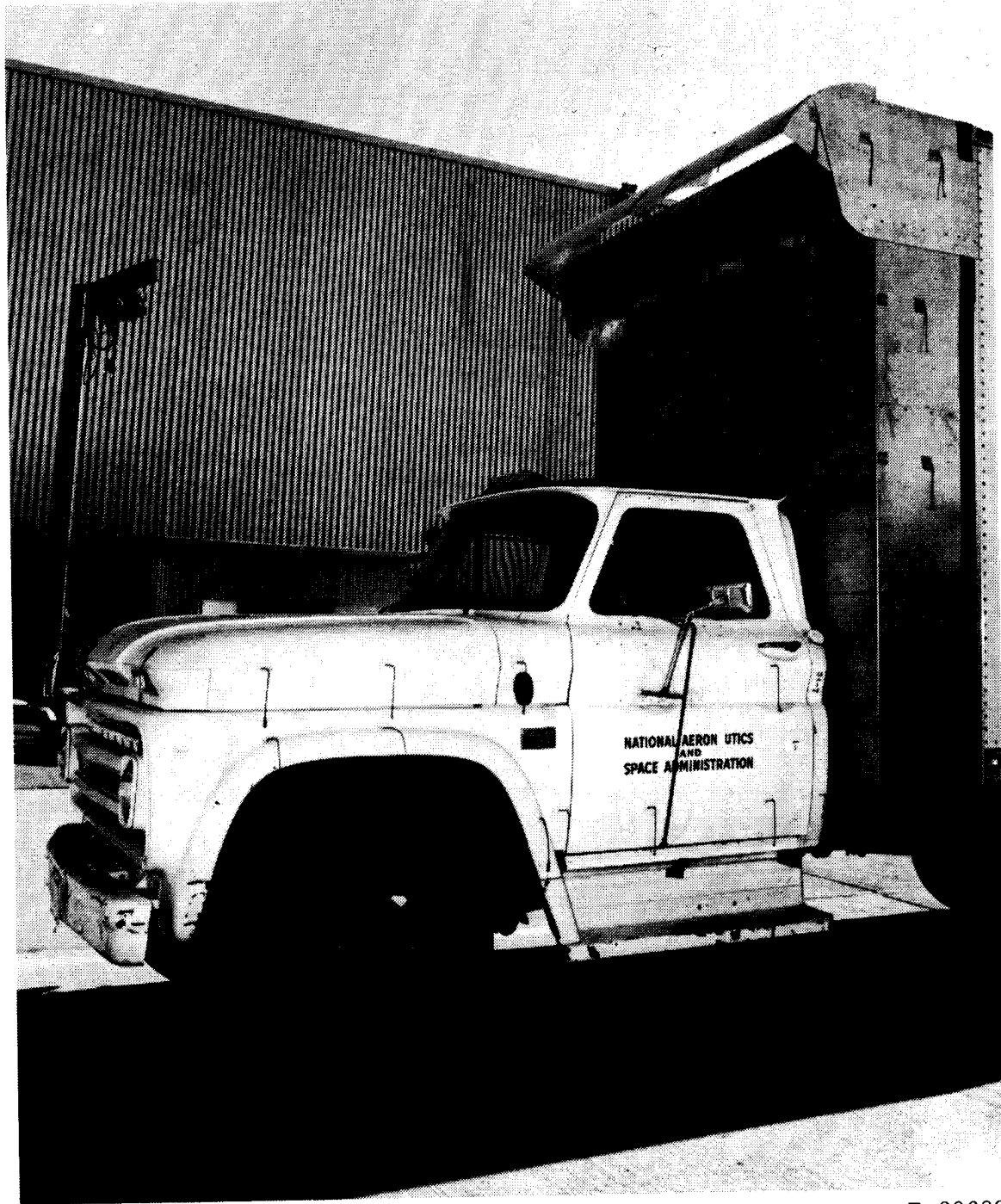


Figure 2. Geometric specifications of baseline vehicle. Dimensions are in meters (inches).



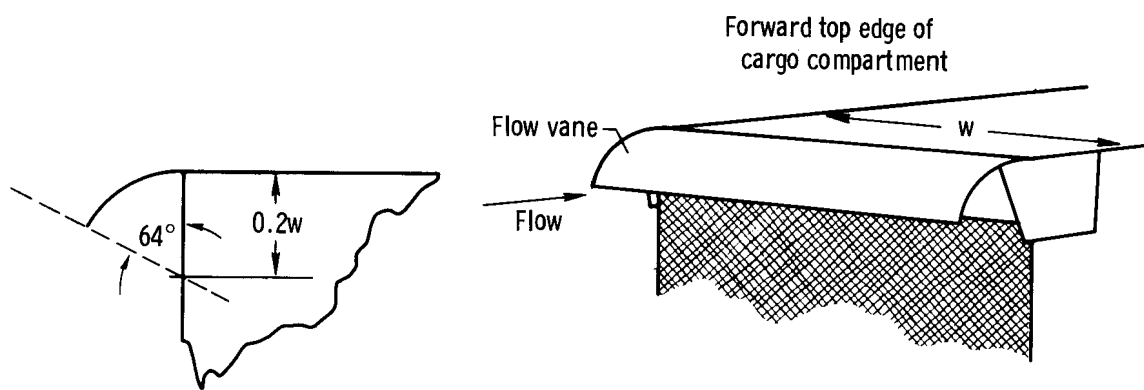
E-30709

Figure 3. Vehicle with rounded edges, configuration B.

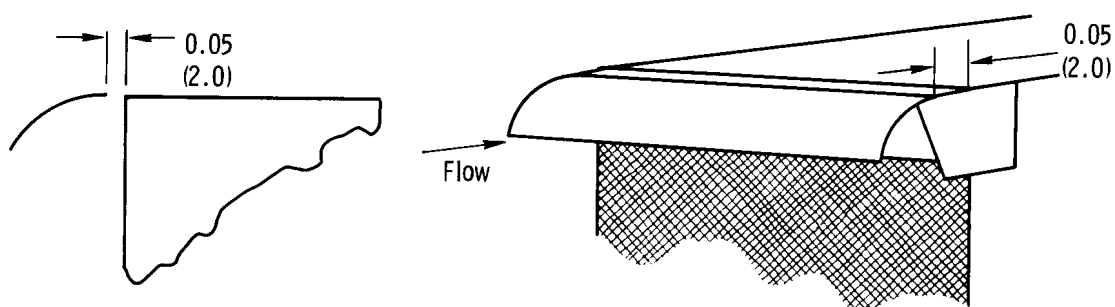


E-29089

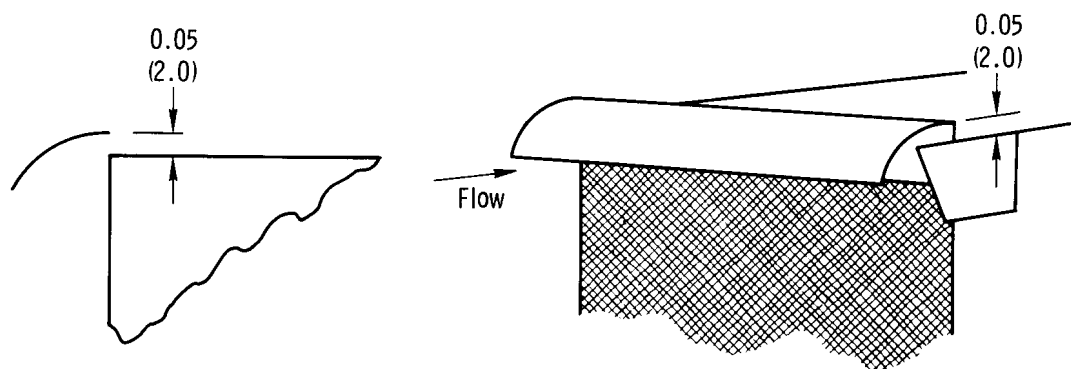
*Figure 4. Location of flow vane on cargo compartment.*



(a) Configuration C.

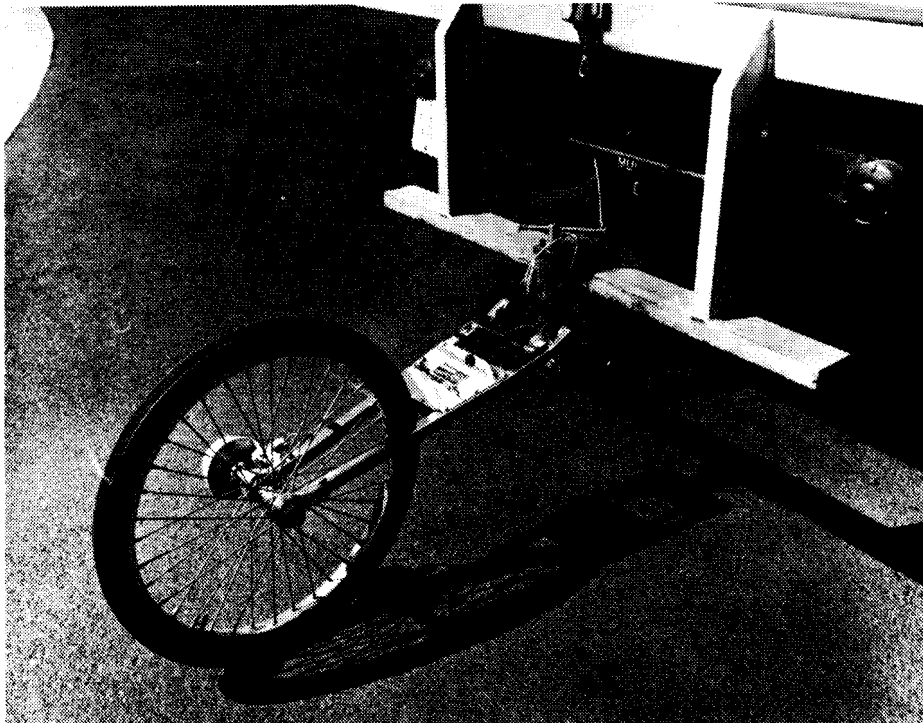


(b) Configuration D.



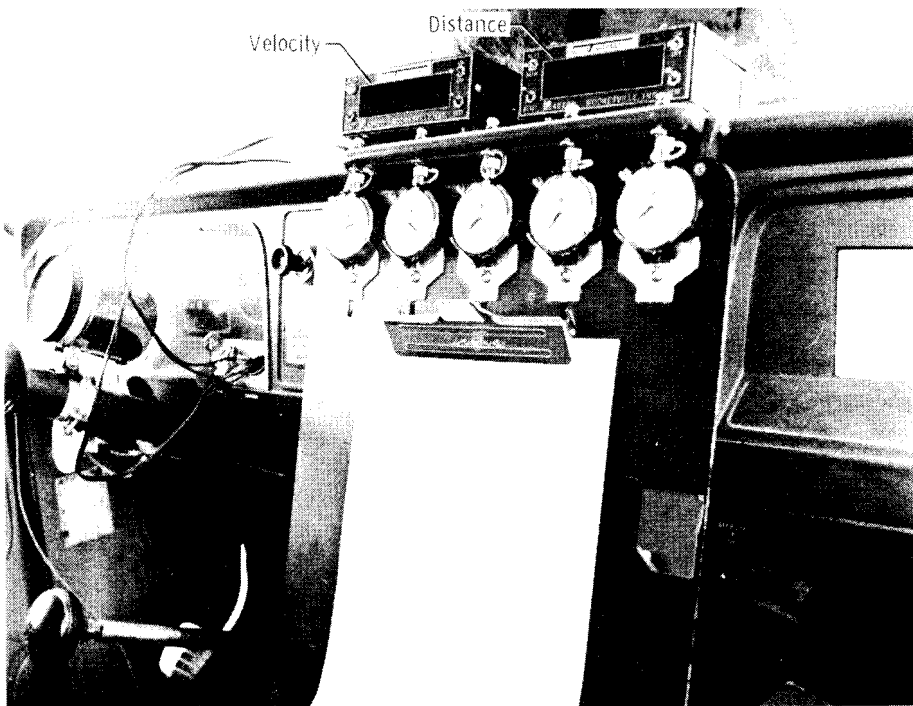
(c) Configuration E.

Figure 5. Flow-vane configurations. Dimensions are in meters (inches).



E-30710

*Figure 6. Calibrated fifth wheel.*



E-30727

*Figure 7. Instrumentation layout inside cab.*



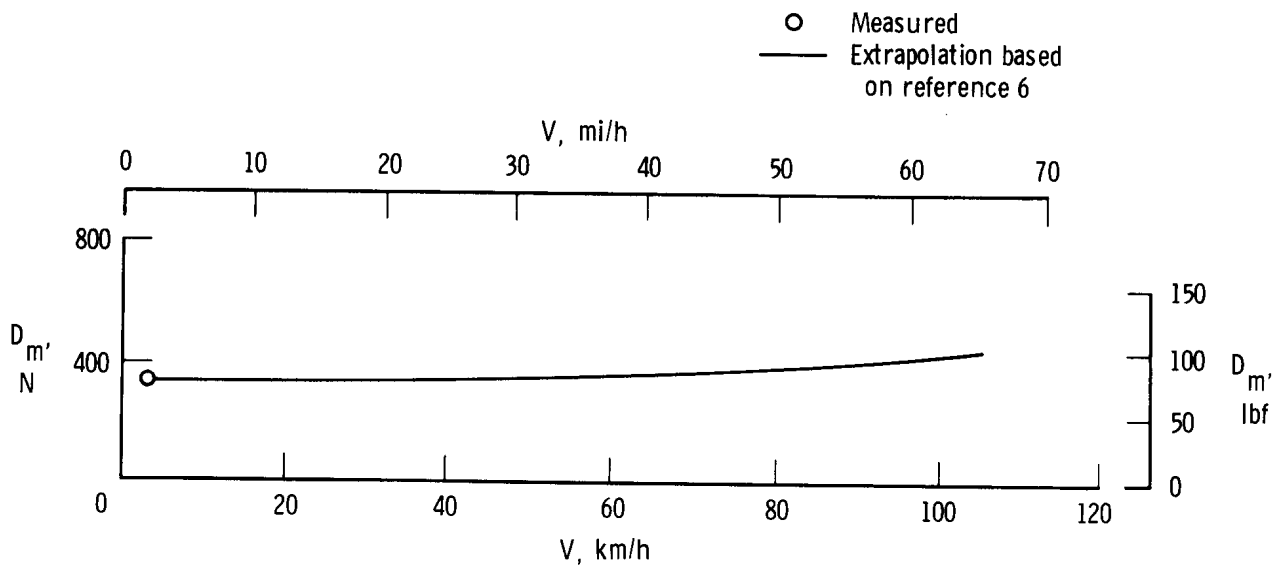


Figure 8. Variation of mechanical drag with vehicle velocity.

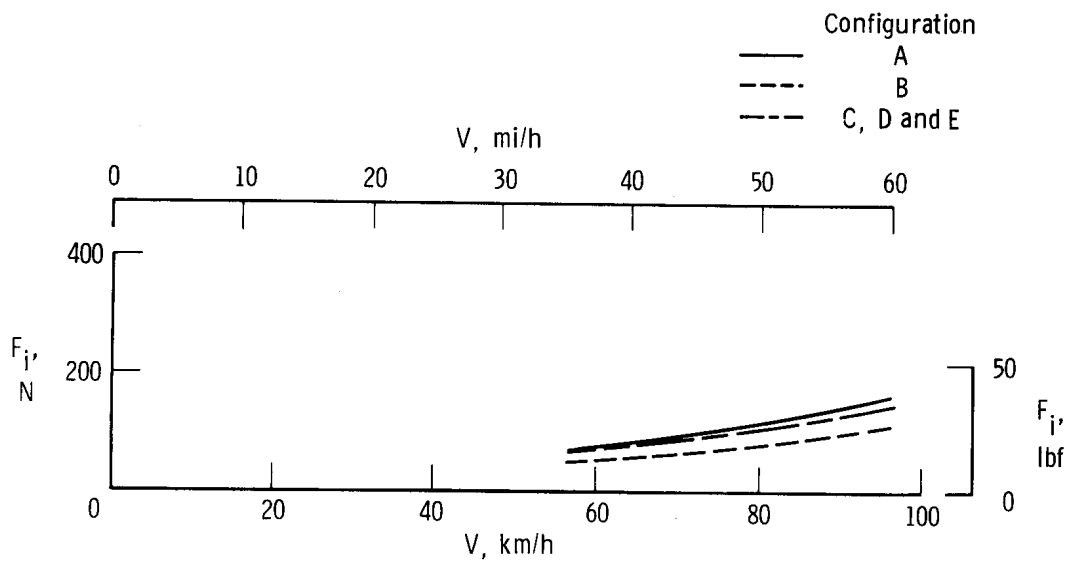
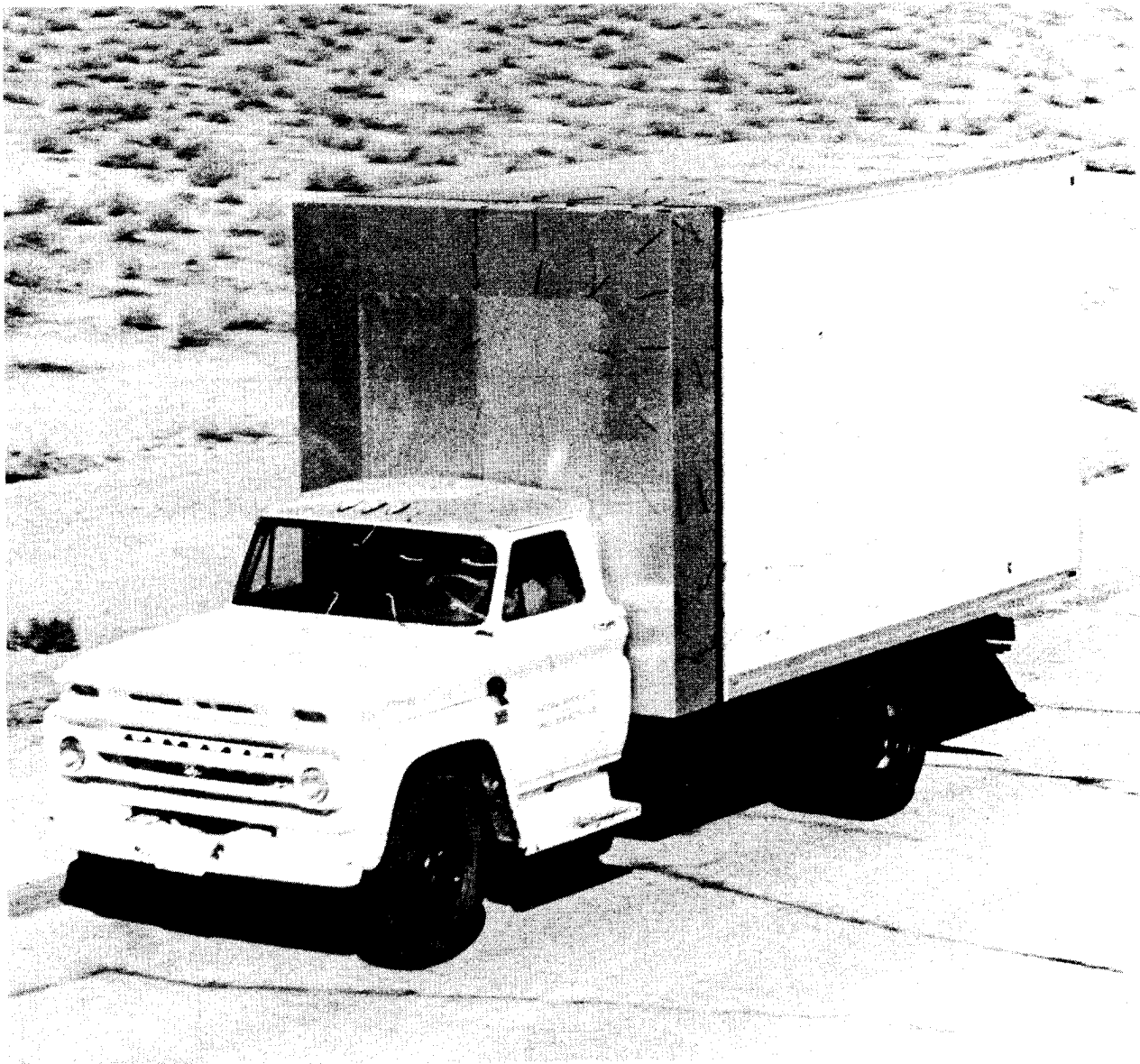


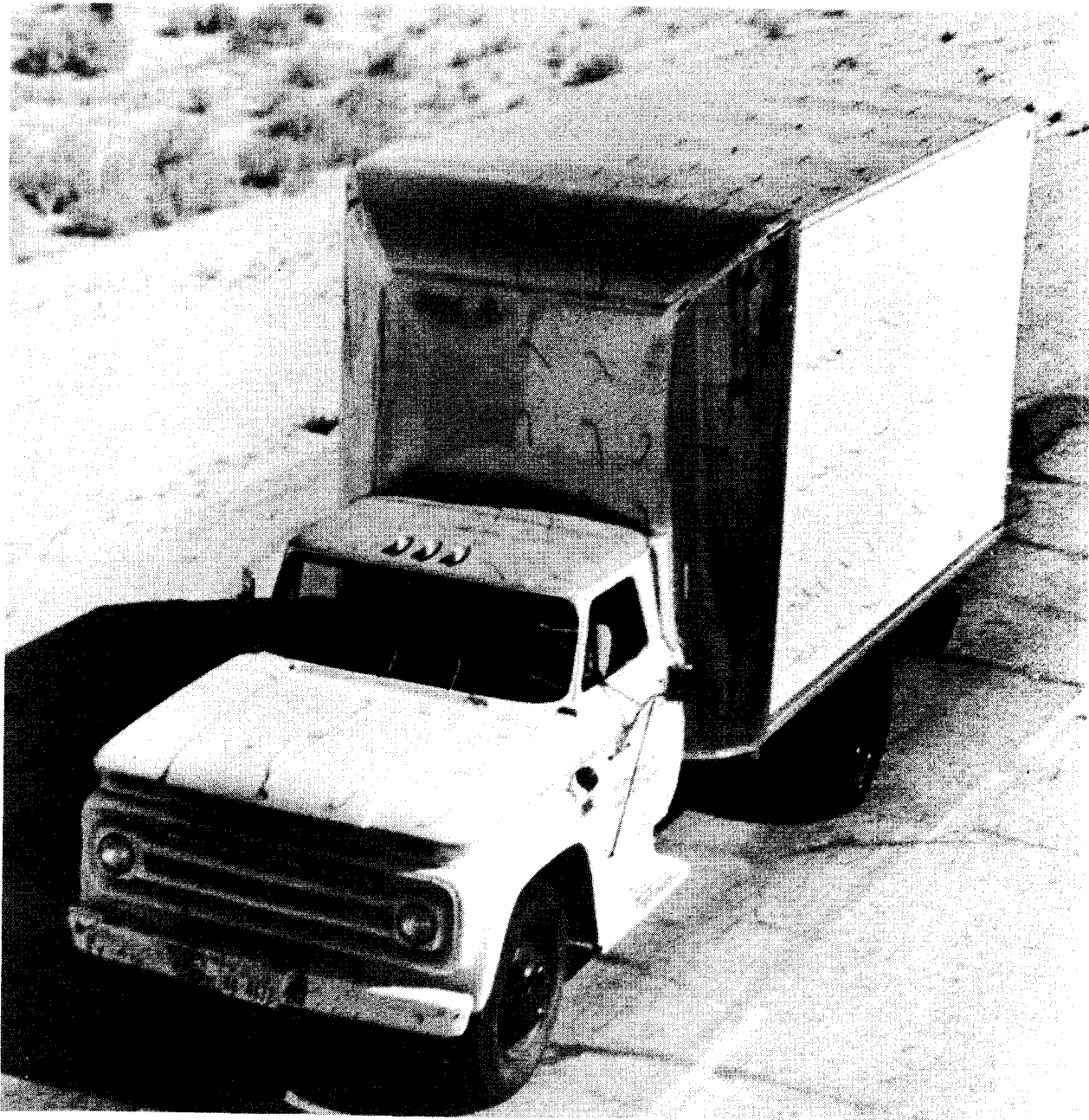
Figure 9. Variation of inertial thrust with vehicle velocity.



E-27965

(a) Configuration A.

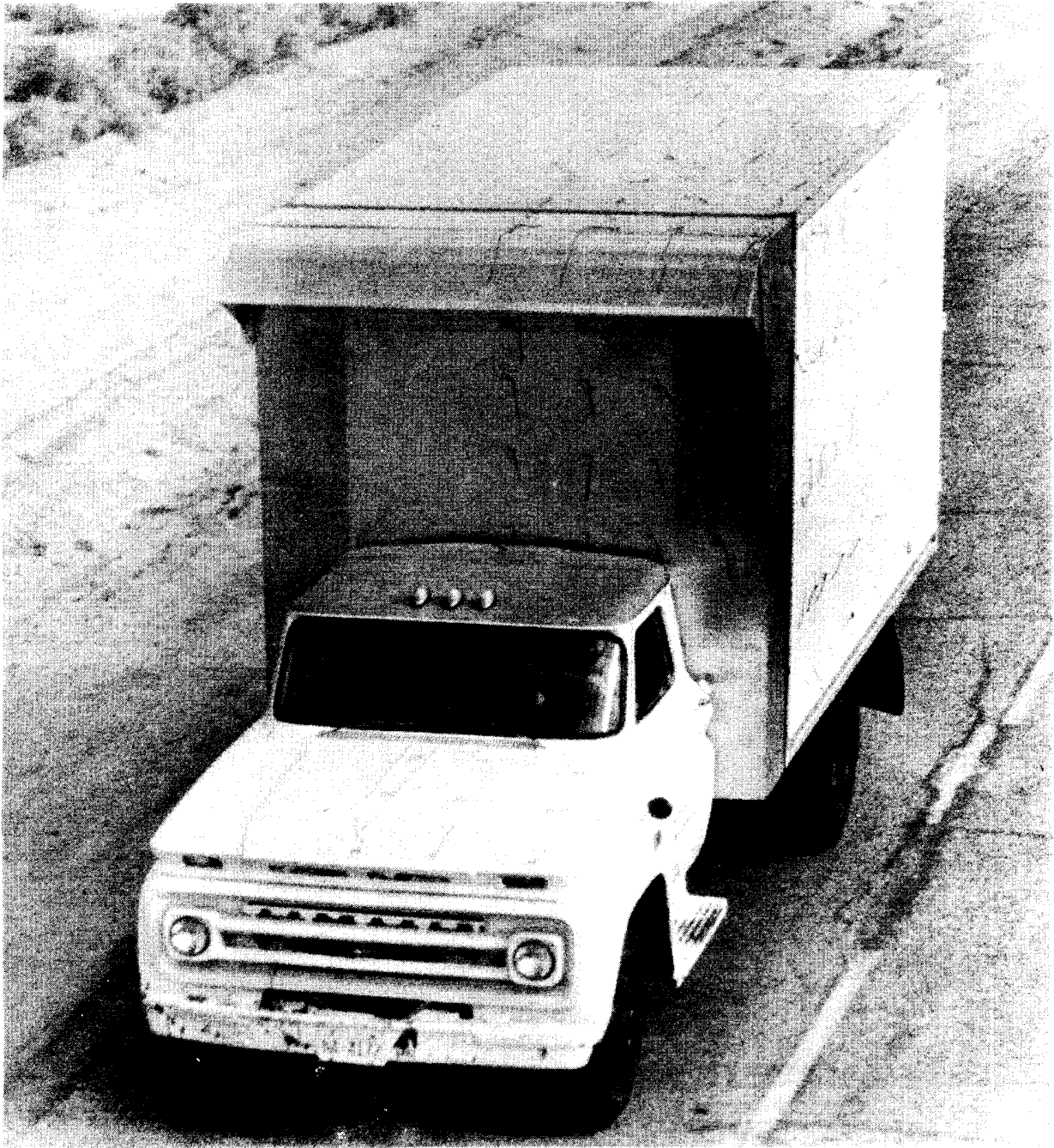
*Figure 10. Tuft patterns at a velocity of 88.5 kilometers per hour (55 miles per hour).*



E-27683

*(b) Configuration B.*

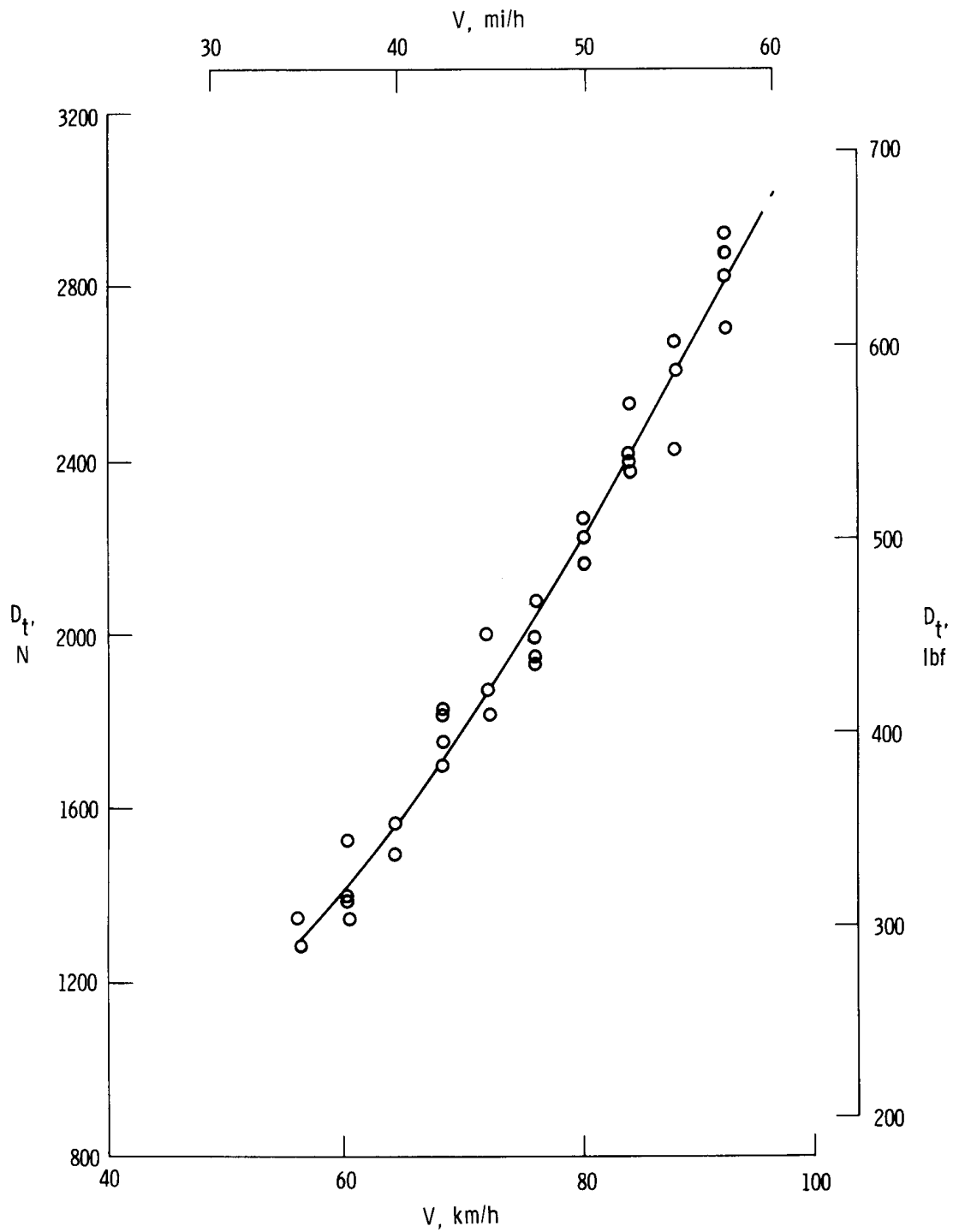
*Figure 10. Continued.*



E-28964

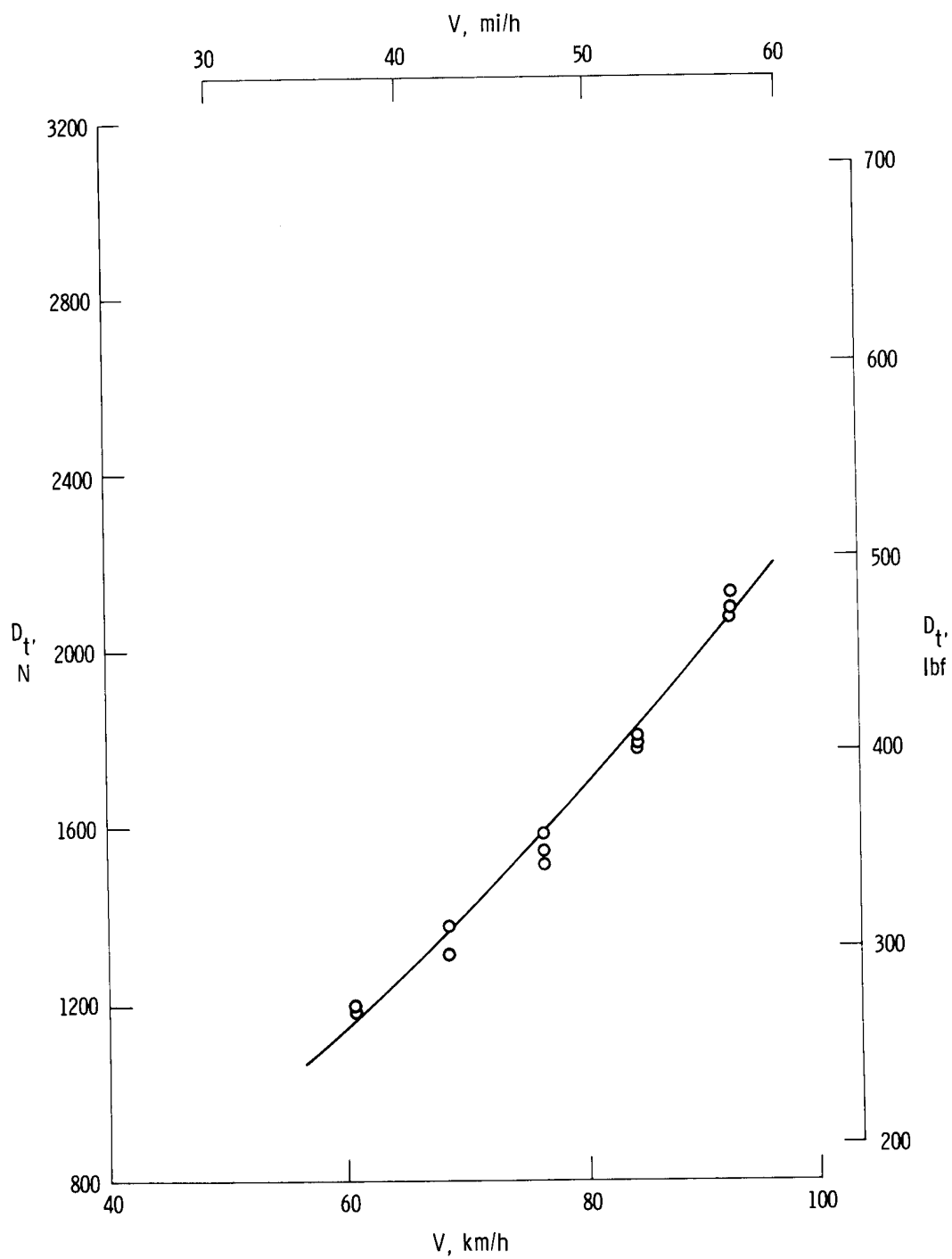
*(c) Configuration D.*

*Figure 10. Concluded.*



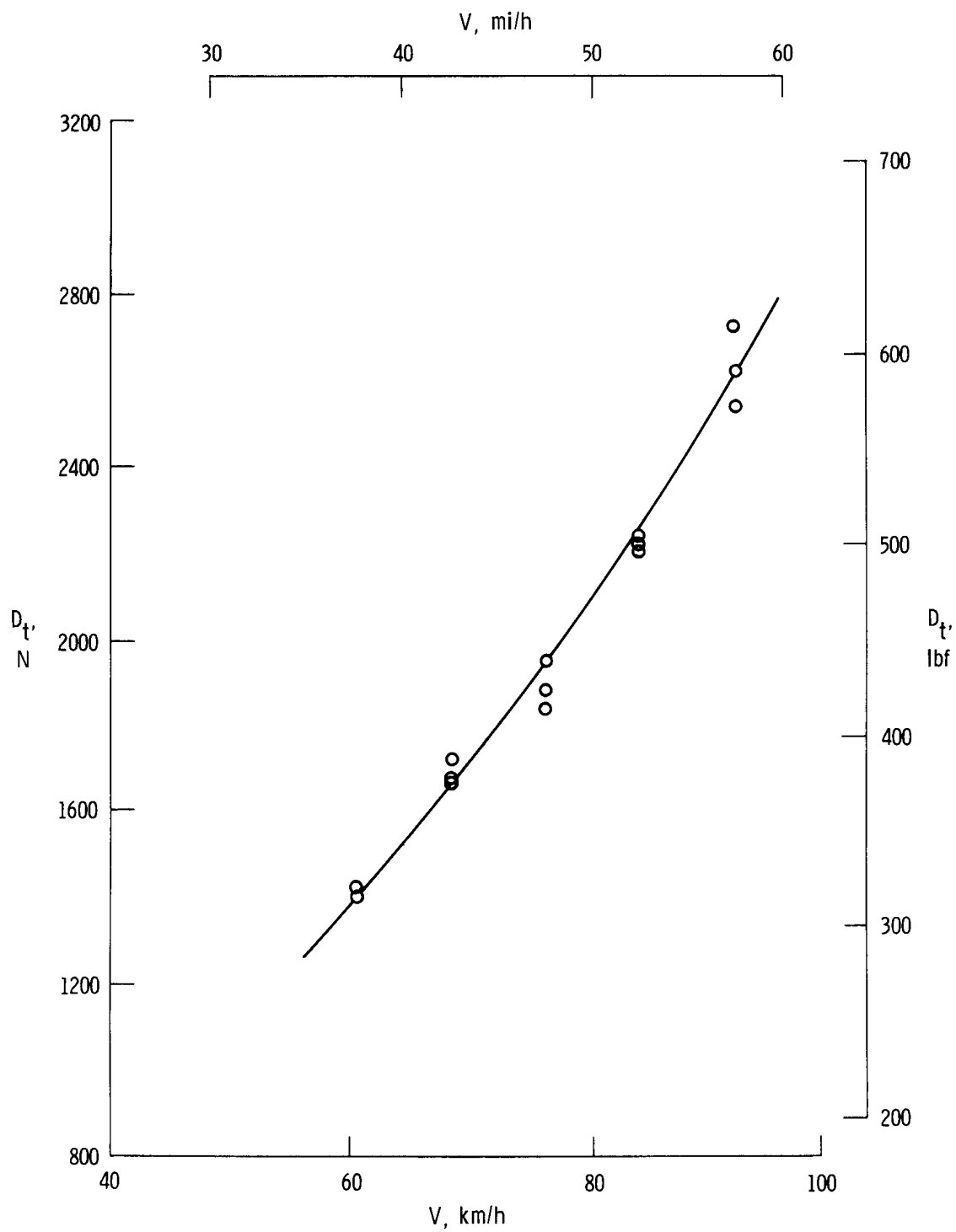
(a) Configuration A.

Figure 11. Variation of total drag with vehicle velocity.



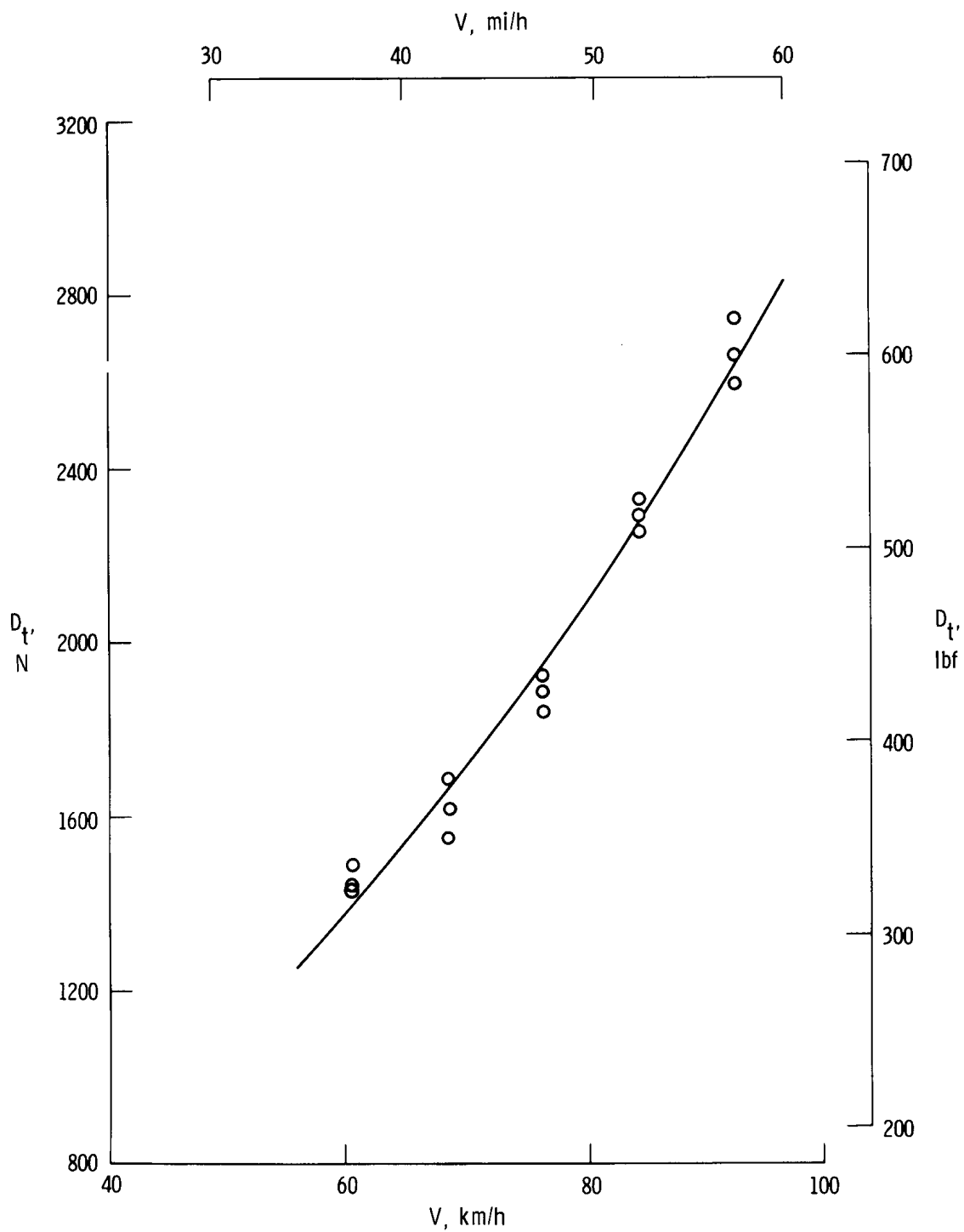
(b) Configuration B.

Figure 11. Continued.



(c) Configuration C.

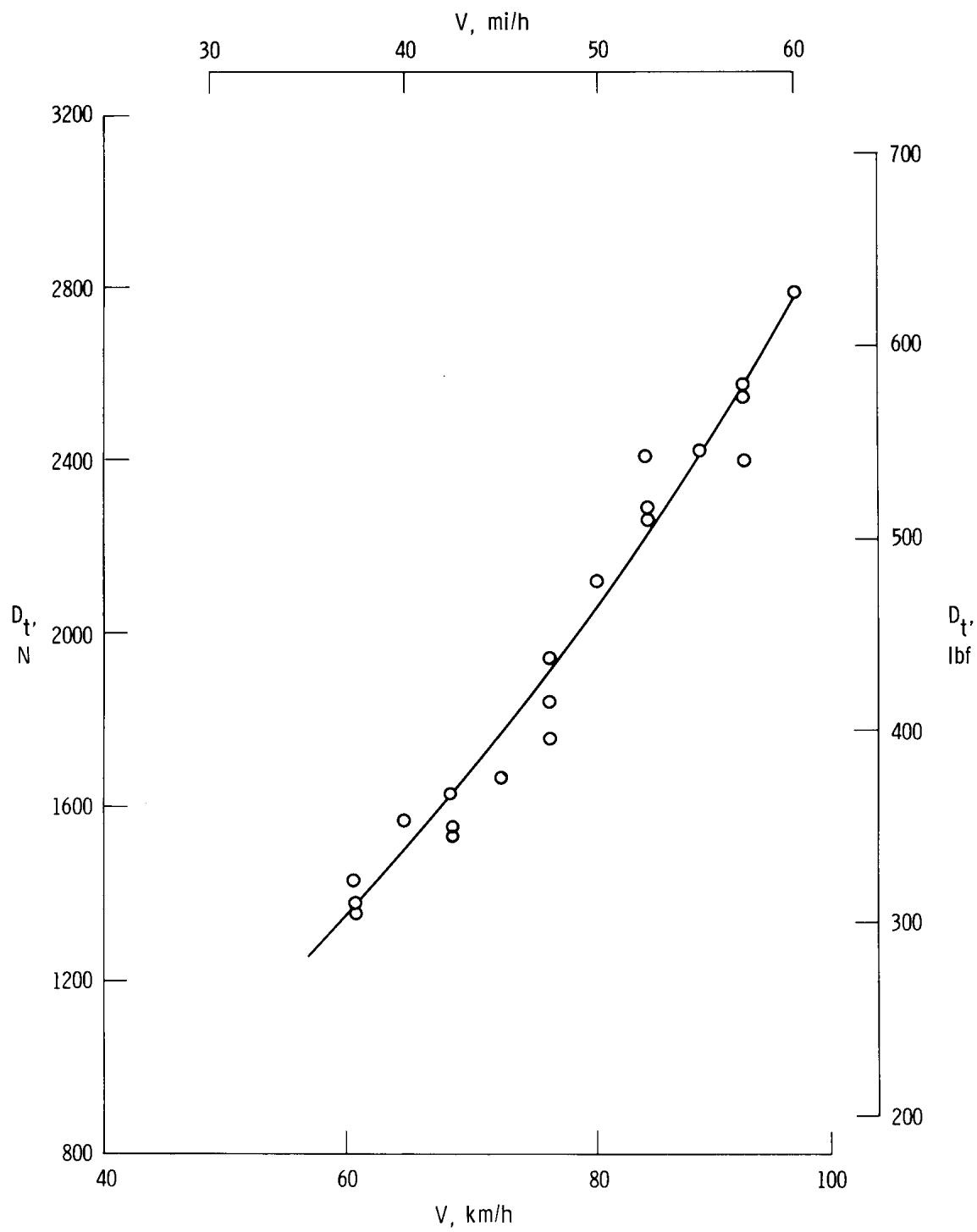
Figure 11. Continued.



(d) Configuration D.

Figure 11. Continued.





(e) Configuration E.

Figure 11. Concluded.

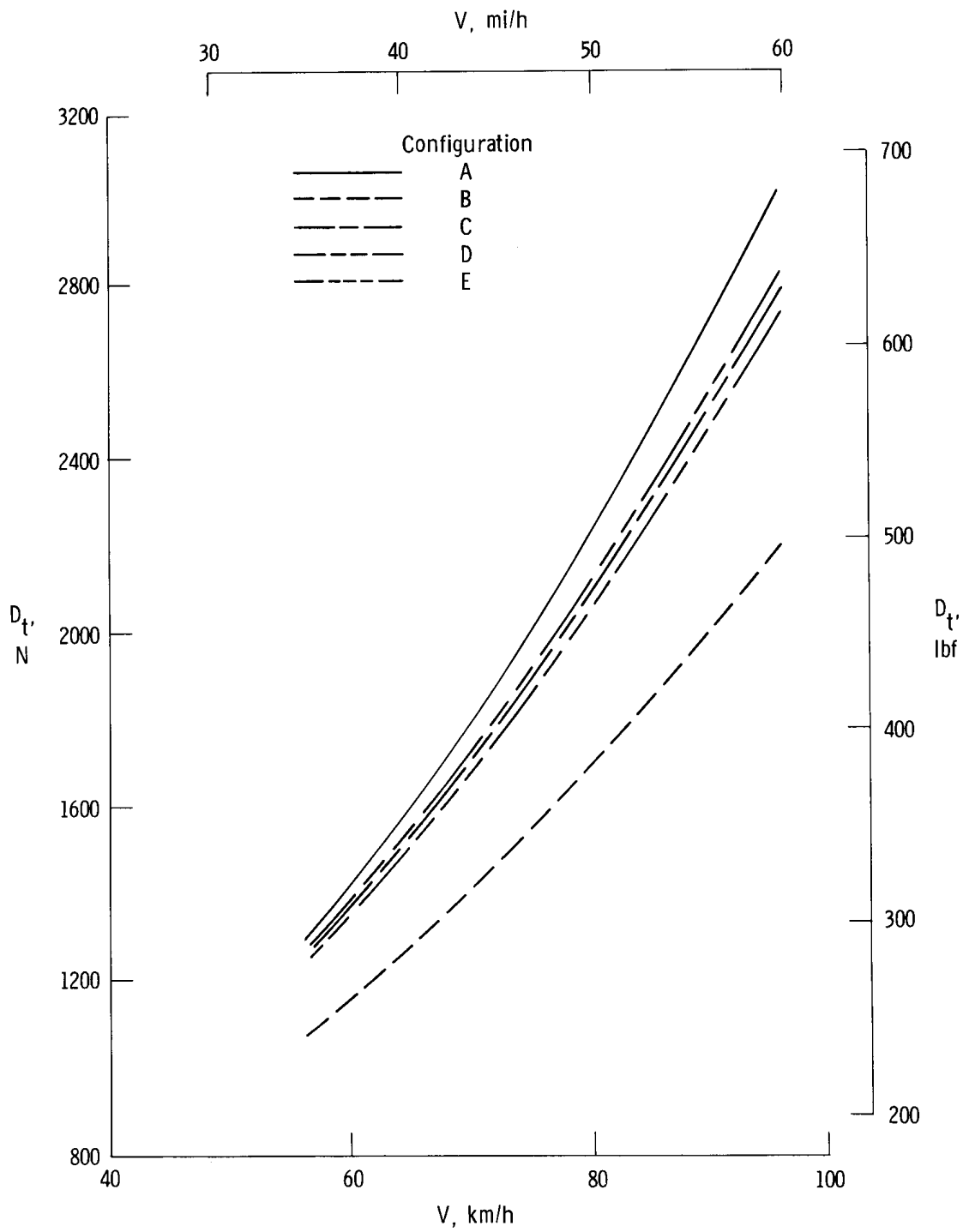


Figure 12. Composite plot of total drag versus vehicle velocity for all configurations.

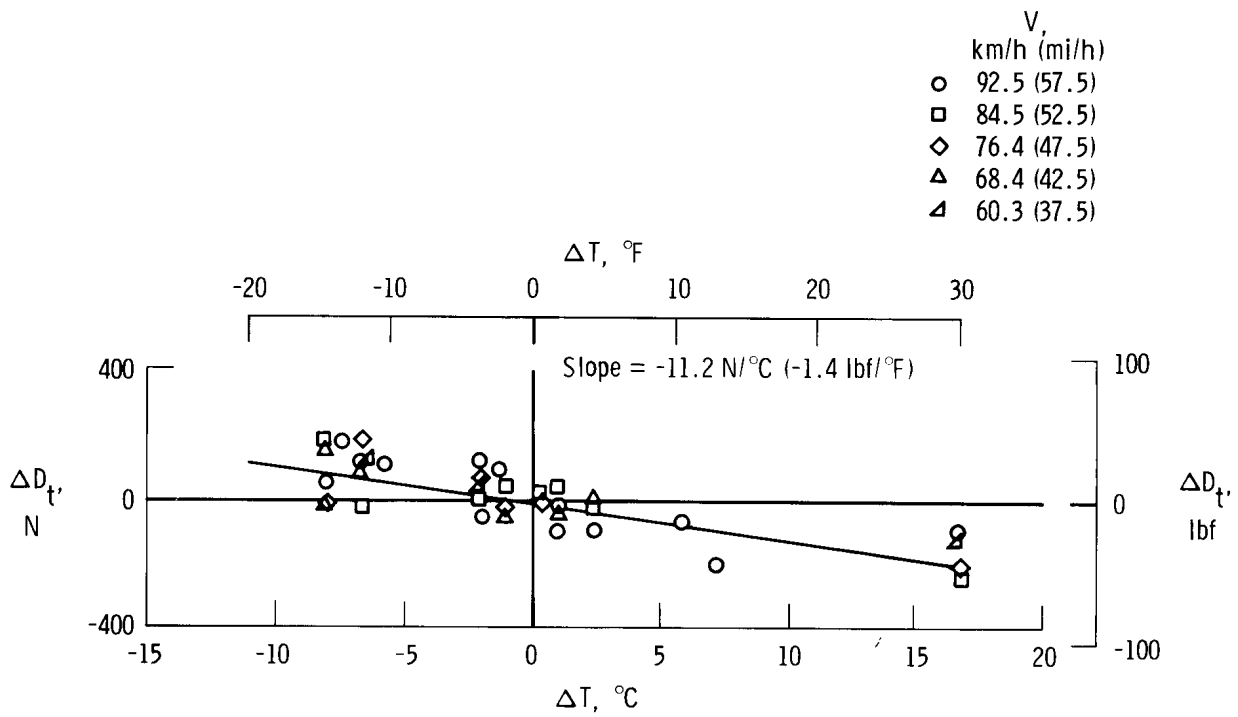


Figure 13. Ambient temperature correction for total drag.

